Chapter 6
Application of Geoinformatics and AHP Technique to Delineate Flood Susceptibility Zone: A Case Study of Silabati River Basin, West Bengal, India

Debasis Ghosh ⓘ**, Monali Banerjee** ⓘ**, Manas Karmakar** ⓘ**, and Dayamoy Mandal** ⓘ

Abstract Among all the natural disasters, floods are the most common phenomena that cause huge obliteration to the human lives and socio-economic and cultural infrastructures. Silabati, a monsoon influenced river of West Bengal is well known for frequent flooding events in its lower basin areas. In the present study, an attempt has been made to delineate flood susceptible areas of Silabati river basin using AHP (Analytical Hierarchy Process) technique and geospatial technology. A total number of 11 physiographic, climatic, and anthropogenic factors (elevation, slope, flow accumulation, distance from river, drainage density, geomorphology, lithology, surface runoff, topographic wetness index, land use land cover, and curvature) are taken into consideration to prepare the flood susceptibility map of the study area. The map is categorized into five distinct flood susceptible zones, such as very high, high, moderate, low, and very low susceptible zones, and these zones cover 14.04%, 20.67%, 21.76%, 20.69%, and 22.84% of the total basin area, respectively. Keshpur, Ghatal, Chandrakona-I, Chandrakona-II, and Daspur-I Community Development (C.D.) blocks of West Medinipur district located in lower Silabati basin fall under very high and high flood susceptibility zones. The performance and efficiency of AHP are validated using Area Under Curve (AUC) method, which ensured significant accuracy (76.41%) of the study. A large number of people residing on lower Silabati basin along with several socio-economic and cultural structures get severely affected many times during floods. Therefore, this study may facilitate the formulation and implementation of flood management strategies in the vulnerable areas of Silabati river basin.

Keywords Geospatial technology · AHP · Causative factors · Flood susceptibility · Silabati river

D. Ghosh (✉) · M. Banerjee · M. Karmakar · D. Mandal
Department of Geography, University of Calcutta, Kolkata, West Bengal, India

97

6.1 Introduction

Flood is the most common among all catastrophic environmental hazards; it causes massive damages to the natural and human resources. In respect to the human society, flood is the most devastating natural hazard because of its irreversible damage capacity to infrastructure, life loss, loss of agricultural, social disruption, etc. (Taylor et al., 2011; Dawod et al., 2011; Swain et al., 2020). The low-lying regions of the world are mostly facing the terrible form of floods due to water logging for incessant rainfall, exhaust of water beyond the carrying capacity of the stream, settlement in the front of swirling water, etc. (Ghosh & Kar, 2018; Natarajan et al., 2021). Globally, on an average, 170 million people are adversely affected by flood every year (Kowalzig, 2008; Das, 2019). In between 1998 and 2017, more than two billion people are affected due to the devastation caused by flood events across the world (World Health Organization, 2018), and 656 million USD economic loss with more than 1.4 lakh human life loss have occurred during this time span (Wallemacq & Rowena, 2018). A total number of 4731 people have lost their lives across the world only in floods occurred in 2016, where average annual death (2006–2015) in flood is 5709 people (Guha-Sapir et al., 2016; Chowdhuri et al., 2020). According to world disaster report (2015), Asia recorded highest number of affected and dead people due to flood around the world in between 2005 and 2014 (World Disasters Report 2015). Most of the developing countries of Asia bear the devastating results of flood, such as China, India, Pakistan, Bangladesh, Sri Lanka, Indonesia, etc. (Wallemacq & Rowena, 2018). In India, every year since 1953 to 2016, 7.19 million hectare area and 31.88 million people on an average are affected by flood. During this time period due to flood India has suffered a loss of 347,581.201 crore rupees and the increasing trend of loss with years is going on (Flood Damage Statistics, 2018). In 2017, a total number of 868 people lost their lives by flood during mid of august (Hindustan Times, 2017a). In the next year (August 2018) a massive flood hit Kerala, where 1.24 million people dislocated and 474 people died (Sphere India, 2018). This terrible scenario of adverse effects of flood does not change very much for West Bengal. The flood damage statistics of 2018 revealed that around 244.23 million people of West Bengal are affected by floods occurs in between 1953 and 2016, and the state has suffered with a loss of 43,954.792 crore rupees (Flood Damage Statistics, 2018).

Floods in India are mainly occurred because of natural (heavy monsoonal rainfall, cyclone, cloud blast, etc.) and manmade (large dam, siltation of river, sand mining, unsystematic management of drainage, etc.) factors (Şen, 2018; Chowdhuri et al., 2020; Sarkar & Mondal, 2020). In India, rural areas are facing huge agricultural loss, occasional loss of livestock and human life, etc. and urban areas are suffering with losses of domestic assets and infrastructures due to inundation of flood plain of the river, costal area, etc. (Şen, 2018). This amount of losses and damages from floods are increasing every year in relation with increasing trends of flood frequency (Flood Damage Statistics, 2018). In the previous two decades, the frequency of floods has increased by 40% worldwide (Hirabayashi et al., 2013; Khosravi et al., 2019).

Therefore, impeding an increase in loss and damages by flood are essential for the sake of human society and environment (Jongman, 2018; Genovese & Thaler, 2020). The analysis of flood events is very significant to reduce the potential damages of floods (Huang et al., 2008; Samanta et al., 2018). Pre-flood measure, flood forecasting, post-flood measures are the impost steps of flood analysis (Wanders et al., 2014; Chowdhuri et al., 2020). The first step of flood mitigation is the identification of flood vulnerable zone, which helps to forecasting the flood events (Sanyal & Lu, 2003). Therefore, flood susceptibility mapping is the important part of flood hazard mitigation system, and it is very useful for early warning system, mitigation of future floods events, reducing causalities, etc. (Tehrany et al., 2015; Ali et al., 2019; Sarkar & Mondal, 2020). The susceptibility of flood is determined by several geographical and flood influencing factors, such as geomorphology, geology, rainfall, slope, elevation, land use land cover, drainage density, flow accumulation, etc. (Kazakis et al., 2015; Das, 2018; Hong et al., 2018; Das, 2019). All these factors are analyzed to assess the flood susceptibility zones. Various researchers from different field have adopted different kinds of mathematical and statistical techniques to analyze these factors, such as Analytical Hierarchy Process (AHP) (Das, 2018; Ali et al., 2019; Yousuf Gazi et al., 2019: Jabbar et al., 2019), Frequency Ratio (FR) (Khosravi et al., 2016; Lee et al., 2018; Ali et al., 2019; Liuzzo et al., 2019; Rahman et al., 2019; Sarkar & Mondal, 2020), Logistic Regression (LR) (Pradhan, 2010; Tehrany & Jones, 2017; Lee et al., 2018; Liuzzo et al., 2019; Rahman et al., 2019), Evidential Belief Function (EBF) (Shafapour Tehrany et al., 2019b; Chowdhuri et al., 2020), Artificial Neural Network (ANN) (Jahangir et al., 2019; Rahman et al., 2019), Analytic Network Process (ANP) (Dano et al., 2019), Shannon's Entropy (SE) (Haghizadeh et al., 2017; Liuzzo et al., 2019), Statistical Index (SI) (Shafapour Tehrany et al., 2019a), Weight of Evidence (WoE) (Khosravi et al., 2016; Rahmati et al., 2016), and Support Vector Machine (SVM) (Tehrany et al., 2015, 2019b), etc. All the models have some advantages and limitations; thus, selection of best model for flood susceptibility is a tough work. The most favorable and preferred multi-criteria decision-making technique is the AHP techniques for flood susceptibility mapping, and a wide number of researchers have already adopted AHP with adequate accuracy (Lawal et al., 2012; Matori et al., 2014; Elkhrachy, 2015; Ghosh & Kar, 2018; Yousuf Gazi et al., 2019; Hammami et al., 2019; Hoque et al., 2019; Jabbar et al., 2019; Phrakonkham et al., 2019; Rahman et al., 2019; Vojtek & Vojteková, 2019; Mishra & Sinha, 2020; Subbarayan & Sivaranjani, 2020; Chakraborty & Mukhopadhyay, 2019). In this technique, the impact of flood provoking factors is assessed by the application of pair-wise comparison matrix and ranked all the factors to delineate priorities zones (Vojtek & Vojteková, 2019; Swain et al., 2020). Enumerating, weight computation, interpolating and integration methods are incorporated in this technique (Chen et al., 2011). In the recent time, the integration of different factor to delineate the susceptible zones of flood is done through the application of Geographical Information System (GIS) and Remote Sensing (RS).

In the recent past, various researchers from different disciplines successfully integrate multi-criteria decision-making tools and GIS for the delineation of flood vulnerable zones, such as Das (2019) worked on flood susceptibility mapping and hydro-geomorphic response to flood. Integrated application of AHP and GIS is used to fulfill the objective; Saha and Agrawal (2020) adopted AHP and GIS technique to assess the flood risk of Prayagraj district, India. In their study, flow accumulation factor is considered as the high influencing factor to food; Sarkar and Mondal (2020) conducted a study on Kulik river basin to delineate the flood vulnerability zone. The FR model has been successfully used to perform the quantification of determination potentiality of causative factors of flood and integrated using GIS platform; Swain et al. (2020) have tried to find out the flood susceptibility zone of a flood vulnerable zone of Bihar using AHP and GIS technique. In their study, a total number of 21 flood causative factors are considered; other studies are Ghosh and Kar (2018); Chowdhuri et al. (2020); Deepak et al. (2020); Natarajan et al. (2021); Malik and Pal (2021); Arya and Singh (2021); etc. So, widely accepted integration approach of AHP and GIS has been used in the present study to find the susceptible zone of flood in Silabati river basin.

In perspective of flood, Silabati river is one of the most vulnerable rivers in south Bengal (Government of West Bengal, 2019). Almost every year overflow of Silabati river causes flood, specifically in the areas of Banka, Khirpai, and Ghatal of lower Silabati river basin (IWAI, 2016; Das et al., 2020). Due to inundation of adjacent areas of Silabati, thousands of people have dislocated and lots of damages have occurred (Hindustan Times, 2017b). In between 1978 and 2016, a total number of 10 high magnitude floods hit the flood plain of Silabati basin (Dandapat & Panda, 2018). During the inundation period, the loss of resources in lower reach of Silabati is maximum (Das et al., 2020). A number of flood hazards have occurred in the recent past years (2011, 2013, 2014, 2015, 2016, and 2017) in Silabati River caused huge damages (NRSC, 2018). The narrow channel of lower Silabati River indulges the overflow of water and causing of embankment breach (Das et al., 2020). This event causing high inundation of area and people suffered with huge agricultural losses, which terrifies the people of several villages (News18, 2019). Additionally, every year some causeways are submerged under the water of Silabati River (Anandabazar Patrika Online, 2020). In this context, flood susceptibility zone delineation and level of vulnerability assessment are very much essential for flood management in Silabati river basin. Considering the flood prone characteristics and adverse effect of flood in Silabati River, the present study was conducted. Thus, the present study tried to find out the flood susceptibility zones of Silabati river basin using AHP and geoinformatics. It will help to provide better forecasting about inundation intensity to the floodplain dwellers and make a positive step in flood management of Silabati river basin.

6.2 Geographical Accounts of Silabati River Basin

The Silabati River is also known as "Silai" which is originated from plateau fringe region of Chota Nagpur plateau and meets with Dwarakeswar River near Ghatal of Paschim Medinipur district, West Bengal. Every year flooding characteristics cannot permit to imagine about the source of Silabati river; it is originated from a pond near Napara village (23°14′09.94″ N and 86°38′42.14″ E) of Puncha community development (C.D.) block of Purulia district. After origin, the river run about 185 km southeasterly and several tributaries, such as Joypanda, Kubai, Tamal, Betal, Parang, Champa, Tarajoli, Mulajor, Purandar and Amoor, etc. enters into the main river channel during it course. The entire Silabati basin covers an area of 4195 km^2 and located Purulia, Bankura and West Medinipur districts of West Bengal, India (Fig. 6.1). The geographical extension of the river basin is 22°23′N to 23°15′N and 86°38′E to 87°46′E. Geomorphologically, the basin is located in between Bengal plateau and stable-self part of Bengal basin. Topography of Silabati river
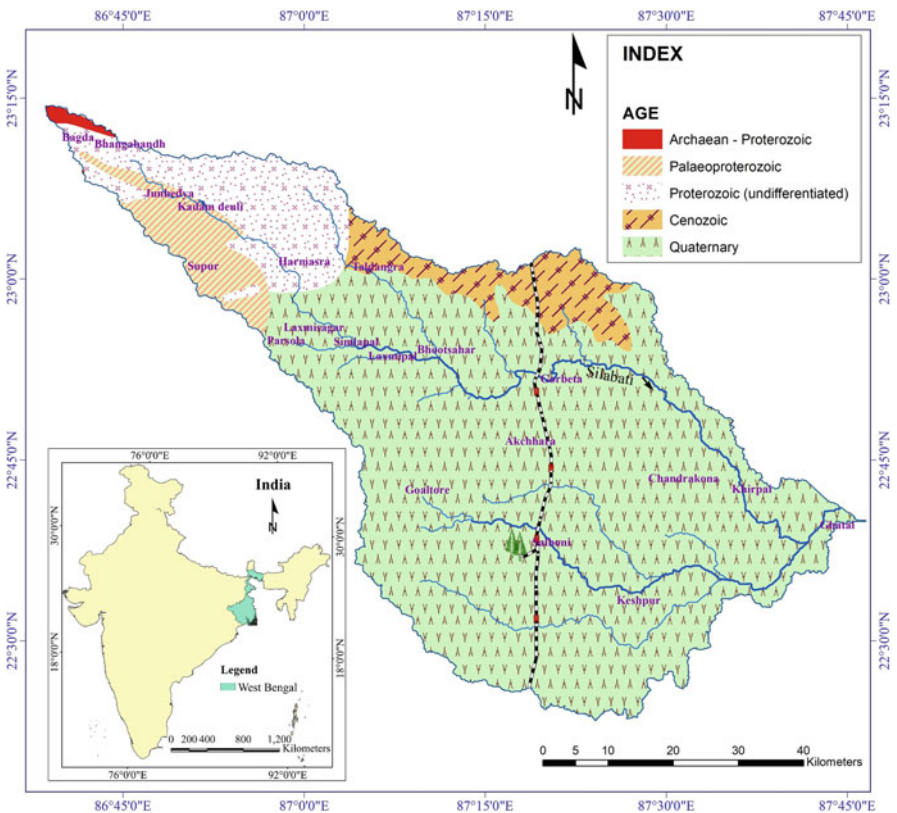

Fig. 6.1 Location map of Silabati river basin. Different symbols used within the basin indicate age of various geological formations. (Source: GSI and Google Earth Image)

basin gradually varies from upper reach (undulating surface of Chota Nagpur plateau) to lower reach (alluvium plain of Ganga delta) (Geological Survey of India, 2001). The isolated hillocks (average 150 m height) are found in the upper part, while isolated highlands are observed at the lower part. The high concentration of lateritic upland of Pleistocene and river flow along this upland formed the famous geomorphosite of West Bengal, i.e., bad land of Gangani (Mandal & Chakrabarty, 2021). The study area experiences sub-humid tropical climatic conditions, and receives annual 100–150 cm rainfall annually (Mahala, 2020). Most of the rainfall is occurred in Monsoon period. Almost in every year, lower reach of the basin encounters flood owing to physiographic characteristics and excessive rainfall over a short time span. It is quite evident from the structures of river bank protection near Talda, Khamardanga, Mathurakata, Gangra, Jhumka and Gugia villages (Bankura district) that the flood occurring nature of the river is very much severe. The important towns within the catchment area are Taldangra and Simlapal of Bankura district; Garbeta, Salboni, and Chandrakona of Paschim Medinipur district.

6.3   Material and Methods

Data Sources

In order to assess the flood risk and vulnerability mapping of Silabati river basin, a total number of 11 flood influencing factors, such as elevation, slope, flow accumulation, distance from river, drainage density, geomorphology, lithology, surface runoff, land use land cover, topographic wetness index, and curvature are taken into consideration. Data set of these selected causative factors is obtained from different types of sources, like Digital Elevation Model (DEM) of Shuttle Radar Topography Mission (SRTM) with spatial resolution of 1 Arc sec (acquired on 23rd September, 2014) downloaded from the United States Geological Survey (USGS) website (https://earthexplorer.usgs.gov); Landsat 8 Operational Land Image (OLI) of 30 m spatial resolution (acquired on 16th May, 2018) obtained from https://earthexplorer.usgs.gov; Topographical Maps (73I/12, 73I/16, 73J/13, 73M/4, 73M/8, 73M/12, 73N/1, 73N/2, 73N/5, 73N/6, 73N/9 and 73N/10) of Survey of India (SOI) on a scale of 1:50,000; District Resource Maps of Geological Survey of India (GSI) on a 1:250,000 scale (Purulia, Bankura and West Medinipur districts); geomorphological map derived from GSI on a scale of 1:250,000; Socio-economic and cultural infrastructures from Google Earth Image; and yearly surface runoff data acquired from https://bhuvan.nrsc.gov.in maintained by National Remote Sensing Centre (NRSC) of Government of India.

Preparation of Geospatial Layers

The flood susceptibility map of Silabati river basin is prepared using the mentioned factors (Fig. 6.2). All these factors are analyzed in geospatial platform, where geospatial layers of all these factors are prepared. The basin map of the study area is delineated from SRTM-DEM using the hydrology tools in ArcGIS software. Before the operation, SRTM-DEM has been projected with Universal Transverse Mercator (UTM), World Geodetic Survey 1984 (WGS-84) 45 North Zone. After the delineation, basin map was rectified with topographical maps. The elevation, slope, flow accumulation, topographic wetness index, curvature and drainage layer of Silabati river basin are also extracted from SRTM-DEM using spatial analyst tools in ArcGIS software. The drainage density map is prepared by using Inverse Distance Weighted (IDW) technique in ArcGIS. In the same way, buffer tools are used to prepare distance from river layer. The land use land cover layer has been prepared from Landsat 8 (OLI) satellite imagery using maximum likelihood algorithm of supervise classification in Erdas Imagine software. Geomorphology and lithology layer of the basin is prepared from geomorphological and geological map of GSI, respectively. The surface runoff layer of Silabati river basin is prepared from runoff data of NRSC and using the interpolation method (IDW) in ArcGIS software. The geomorphological and geological map has been geo-rectified with the UTM, WGS-84, 45N zone and prepared the required maps in ArcGIS 10.3.1 platform. Finally, all thematic layers are classified into five distinct categories following the Jenks natural break method.
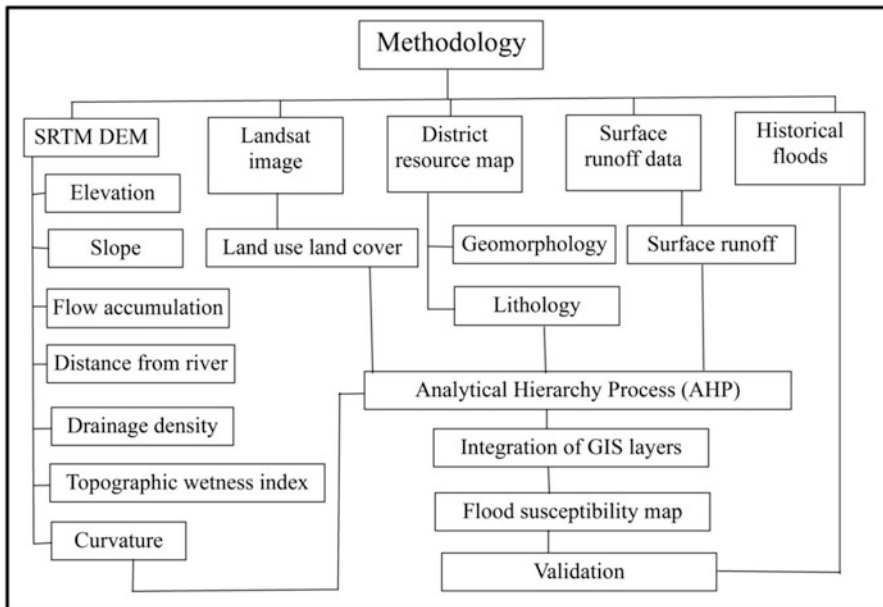

Fig. 6.2 Flowchart of the methodology adopted in the study

Analytical Hierarchy Process (AHP)

All the 11 flood causative factors are interrelated. In the present study, AHP technique is used to quantify the influencing capacity of each factor in flood occurrence through the assigning of weight to each factor (Fig. 6.3). The AHP technique is introduced by Saaty in 1980 (Saaty, 1980). It is a semi-quantitative multi-criteria decision-making approach, in which decisions are made through pair-wise comparison between different factors without inconsistency (Das, 2018; Chowdhuri et al., 2020; Ghosh et al., 2020a; Karmakar et al., 2021). In the field of environmental science several problems have severe complexity and it can be reduced by the application of AHP technique (Kannan, 2010; Çelik, 2019; Arya & Singh, 2021). Another advantage of the technique is the quantification of influencing factor by assigning weight for factor based on the relative importance of factor (Maity & Mandal, 2019; Waris et al., 2019; Ghosh et al., 2020a). In this method, weight assignment is done on the basis of expert judgment of decision makers, and assessment of consistency of judgment value by consistency index (CI) is the strongest part of the method (Das, 2019; Murmu et al., 2019; Karmakar et al., 2021). In this work, the AHP is consisted of two major parts, such as evaluation of causative factors and assign weight and integration of all these factors to compute flood susceptibility index. The evaluation of factors has been done in four steps. In the beginning, weight of each factor is assigned from the literature review, field visits, and expert judgments. Using the nine-point scale of Saaty weight of each factor is assigned based on the relative importance of a factor on the occurrence of

Fig. 6.3 Flowchart of analytical hierarchy process
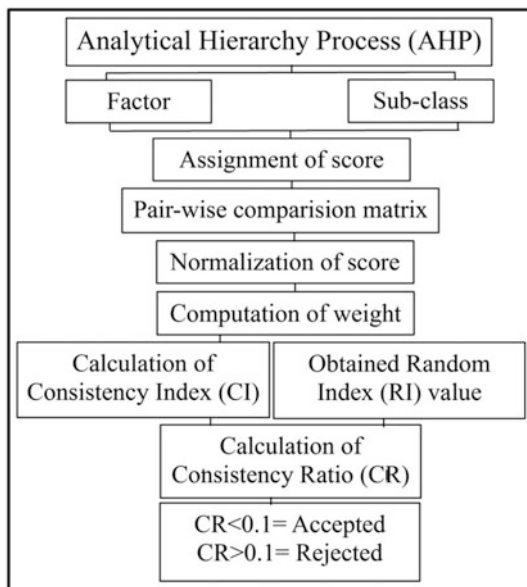
flood (Table 6.1). In the next step, comparison of all factors with each other is done by a matrix which is known as pair-wise comparison matrix (Eq. 6.1).

$$W = \begin{vmatrix} v_{11} & v_{12} & \cdots & v_{1n} \\ v_{21} & v & \cdots & v_{2n} \\ \cdots & \cdots & \cdots & \cdots \\ v_{n1} & v_{n2} & \cdots & v_{nn} \end{vmatrix} \tag{6.1}$$

Here, W is the pair-wise comparison matrix, v is the assign weight of ith factor. In this matrix, assignment of weight depends on the importance of the factor compare to other factor. Thus, the greater influence factor has been assigned to absolute number (Table 6.1) as weight per requirement and less importance factor assigned reciprocal of the absolute number in relation of the greater influence factor. The pair-wise comparison matrix is shown in Table 6.2. After that, estimated Eigen value of each factor is calculated from the matrix table (Table 6.2) by multiplying of all assigned weight of all factors in a row and then the Nth root of the product result is computed by using the Eq. (6.2).

$$EE = \sqrt[N]{V_a \times V_b \times V_c \times \dots V_N} \tag{6.2}$$

Here, EE represent the estimated Eigen value of ith factor; V_a, V_b V_c V_n is the values of the row value of ith factor and N is the total number of factors. The principle Eigen value of each factor is computed using the Eq. (6.3), where Ev denotes the principle Eigen value.

$$Ev = \frac{\sqrt[N]{V_a \times V_b \times V_c \times \dots V_N}}{\sum_{i=1}^{n} EE} \tag{6.3}$$

After the principle Eigen value (λ_{max}) has been calculated, the consistency index (CI) is calculated using the Eq. (6.4). The CI value is divided by the RI value (Eq. 6.5) to compute the consistency ratio (CR) and verify the judgment coherence. The RI value is varying with number of parameter taken into consideration. In the consistency assessment, CR value must be less than 0.1 for acceptance of the judgment value of factor; if not, the pair-wise comparison matrix has to revise with new judgment values and this process will continue until the CR value comes down to less than 0.1 (Saaty, 1990).

$$CI = \frac{\lambda \max - n}{n - 1} \tag{6.4}$$

$$CR = \frac{CI}{RI} \tag{6.5}$$

Table 6.1 Nine-point scale of Saaty and Random consistency index

Scale of importance	1	2	3	4	5	6	7	8	9
Definition	Equal	Weak	Moderate	Moderate plus	Strong	Strong plus	Very strong	Very very strong	Extreme
Number of factors	1	2	3	4	5	6	7	8	9	10	11
RCI	0	0	0.58	0.90	1.12	1.24	1.32	1.41	1.45	1.49	1.51

Table 6.2 Pair-wise comparison matrix of causative factors

Factors	Curvature	Land use land cover	Topographic wetness index	Surface runoff	Lithology	Geomorphology	Drainage density	Distance from river	Flow accumulation	Slope	Elevation
Curvature	1	1/2	1/3	1/4	1/5	1/5	1/6	1/6	1/7	1/8	1/9
Land use land cover	2	1	1/2	1/3	1/4	1/4	1/5	1/5	1/6	1/7	1/8
Topographic wetness index	3	2	1	1/2	1/3	1/4	1/5	1/6	1/7	1/8	1/8
Surface runoff	4	3	2	1	1/1	1/2	1/3	¼	1/5	1/6	1/6
Lithology	5	4	3	1	1	1/1	1/2	1/3	1/4	1/5	1/6
Geomorphology	5	4	4	2	1	1	1/2	1/3	1/4	1/5	1/6
Drainage density	6	5	5	3	2	2	1	1/2	1/3	1/4	1/5
Distance from river	6	5	6	4	3	3	2	1	1/2	1/3	1/4
Flow accumulation	7	6	7	5	4	4	3	2	1	1/2	1/3
Slope	8	7	8	6	5	5	4	3	2	1	1/3
Elevation	9	8	8	6	6	6	5	4	3	3	1

The CR value of the present study is 0.054, which revealed that a consistency is present in the judgment values. Thereafter, weight is assigned to all sub-classes of each factor and the principle Eigen value is computed by considering same procedure of weight assigning.

Flood Susceptibility Index (FSI)

The flood susceptibility index (FSI) is computed using all the selected flood causative factors. The weighted linear combination method is adopted to calculate the FSI. In this method, weight of each factor is multiplied with the rank of sub-classes. The rank is assigned accordingly to sub-classes based on the weightage value of each sub-class of a factor (Table 6.3). Now, the Eq. (6.6) is used to calculate the FSI, where Ev_i is represented the principle Eigen value of ith factor and r_j is the rank of jth sub-classes of respective ith factor.

$$\text{FSI} = \sum_{i=1}^{n} \left(Ev_i \times r_j \right) \tag{6.6}$$

Finally, FSI value is classified into five distinct classes, very low, low, moderate, high, and very high. Based on this method, all the geospatial layers are integrated in ArcGIS software using the map algebra tool.

Accuracy Assessment

Accuracy assessment or validation of model is an integral part of any decision-making model. Without accuracy assessment, any simulation model is incomplete (Chung & Fabbri, 2003; Ghosh et al., 2020b; Sarkar & Mondal, 2020). There are several techniques used by different researchers across the world to validate the simulation models. However, the application of ground level data for accuracy assessment is the most accurate and convenient technique to validate such a model. In case of flood susceptibility assessment, use of historical data of inundated areas due to flood is also evolved as a significant data set for validation of the flood susceptibility map (Pradhan, 2010; Lee et al., 2018; Ali et al., 2019; Das, 2019). In the present study, a total number of 197 known flood sites are demarcated during the flooding season of 2017 using handheld GPS (Garmin eTrex-20) and inundation area identified from the flood map of 2017 provided by NRSC (collected from https://bhuvan.nrsc.gov.in). In this study, the Area Under Curve (AUC) is considered to evaluate the performance and efficiency of the AHP model. To construct the AUC, resultant flood susceptibility map is classified into 100 classes, and cumulative percentage of flood occurrence in different susceptibility classes is also computed. Based on calculation, the AUC is plotted to validate the model (Fig. 6.17).

Table 6.3 Allocation of weight to the selected parameters and their sub-classes

Factors	Weight	Sub-classes	Consistency ratio	Weight	Rank
Curvature	0.0137	0.33–3.37	0.0542	0.0329	1
		0.11–0.33		0.0636	2
		(−0.11)–0.11		0.1296	3
		(−0.33)–(−0.11)		0.2638	4
		(−2.37)–(−0.33)		0.5100	5
Land use land cover	0.0184	Vegetation	0.0098	0.0951	1
		Agricultural land		0.1599	2
		Build-up area		0.2777	3
		Water body		0.4671	4
Topographic wetness index	0.0222	4.19–7.73	0.0542	0.0329	1
		7.73–9.66		0.0636	2
		9.66–11.94		0.1296	3
		11.94–15.39		0.2638	4
		15.39–25.67		0.5100	5
Surface runoff (mm/day)	0.0372	93.70–109.26	0.0155	0.0615	1
		109.26–118.98		0.0975	2
		118.98–127.49		0.1602	3
		127.49–137.70		0.2634	4
		137.70–155.70		0.4174	5
Lithology	0.0476	Chota Nagpur gneissic complex	0.0066	0.1089	1
		Singhbhum group of rock		0.1089	1
		Unclassified metamorphic rock		0.1089	1
		Newer alluvium		0.2008	2
		Older alluvium		0.4724	3
Geomorphology	0.0521	Denudational hill and valley	0.0418	0.0271	1
		Pediment–pediplain complex		0.0510	2
		Older alluvial plain		0.1114	3
		Older flood plain		0.1114	3
		Active flood plain		0.2420	4
		Water body		0.4571	5
Drainage density (km/km²)	0.0764	0.12–0.23	0.0358	0.0377	1
		0.23–0.29		0.0643	2
		0.29–0.34		0.1155	3
		0.34–0.40		0.2667	4
		0.40–0.50		0.5157	5
Distance from river (km)	0.1059	>2	0.0299	0.0419	1
		1.5–2		0.0730	2
		1–1.5		0.1317	3

(continued)

Table 6.3 (continued)

Factors	Weight	Sub-classes	Consistency ratio	Weight	Rank
		0.5–1		0.2398	4
		<0.5		0.5135	5
Flow accumulation	0.1492	0–168,106	0.0058	0.0427	1
		168,106–616,390		0.0750	2
		616,390–1,456,922		0.1429	3
		1,456,922–2,484,239		0.2697	4
		2,484,239–4,744,336		0.4696	5
Slope (degree)	0.1983	4.83–28.67	0.0111	0.0434	1
		3.15–4.83		0.0756	2
		1.91–3.15		0.1427	3
		0.67–1.91		0.2694	4
		0–0.67		0.4690	5
Elevation (m)	0.2784	137–227	0.0111	0.0434	1
		96–137		0.0756	2
		66–96		0.1427	3
		37–66		0.2694	4
		6–37		0.4690	5

6.4   Results and Discussion

Elevation

In general, low laying areas are more prone to flood than elevated areas (Nakajima & Umeyama, 2015). Thus, elevation is the prime factor for determining of flood susceptible areas (Das, 2018, 2019; Janizadeh et al., 2019). Flat low land area tends to have higher vulnerability to inundation than the area located at higher elevation (Das, 2018; Ali et al., 2019; Khosravi et al., 2016; Liuzzo et al., 2019; Rahman et al., 2019; Sarkar & Mondal, 2020; Vojtek & Vojteková, 2019). The prepared elevation map of Silabati river basin shows that the elevation varies from 6 to 227 m (Fig. 6.4). The highest elevation is found in the north-western part of the basin, and continuously decreases towards the south-east direction. The category of elevation of 37–66 m dominates the river basin with a share of 29.10% area followed by 6–37 m (27.38%) and 66–96 m (25.49%).
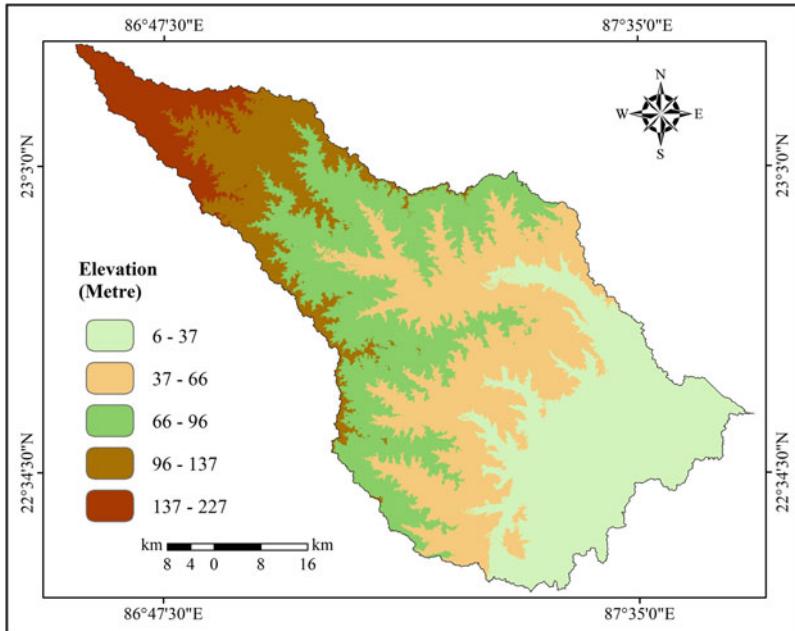
Fig. 6.4 Elevation map of Silabati river basin. (Source: SRTM DEM)

Slope

Slope refers to the amount of inclination of surface in respect to horizontal plane. This factor plays a crucial role in controlling surface runoff, infiltration process, and sub-surface flow (Ali et al., 2019; Das, 2018; Hammami et al., 2019). An area with gentle slope makes itself more vulnerable during flood as flat terrains are more susceptible to water stagnation compared to the area under steep slope (Hammami et al., 2019; Periyasamy et al., 2018). It is observed from the slope map that the slope ranges from 0° to 28.67° in the study area (Fig. 6.5). An area of 47.63% of the river basin experiences slope in between 0.67° and 1.91° followed by 1.91° to 3.14° (24.17%), and only an area of 1.19% belongs to the slope category of 4.83–28.63°.

Flow Accumulation

Flow accumulation is the concentration of flow in a pixel draining out from neighboring pixels (Das, 2018, 2019; Vojtek & Vojteková, 2019). Generally, flow accumulation is observed to be higher and lower in lower reach and upper reach, respectively, in a basin, since stream order and flow accumulation are positively
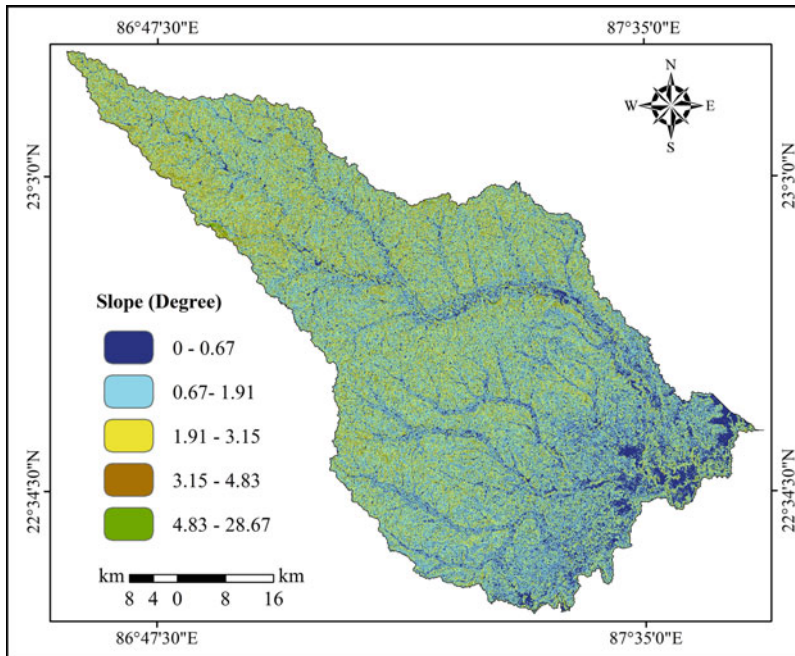
Fig. 6.5 Distribution of slope in Silabati river basin. (Source: SRTM DEM)

correlated (Das, 2018). An increase in flow accumulation enhances the propensity of flood risk (Vojtek & Vojteková, 2019). In this study, highest flow accumulation is seen in the lower reach of the basin due to flat terrain and very gentle slope (Fig. 6.6).

Distance from River

Distance of an area from an active channel is very significant in the field of flood risk mapping (Das, 2018). Areas near the active channels are more vulnerable to flood (Ali et al., 2019; Yousuf Gazi et al., 2019). Based on the drainage network map, a buffer analysis of active channels is carried out with an interval of 0.5 km using proximity analysis tool in ArcGIS software (Das, 2018). A total amount of 27.40% of river basin area lies within 1 km from the active river channel followed by 23.64% area (within 1–2 km), while 48.96% basin area lies greater than 2 km buffer (Fig. 6.7).
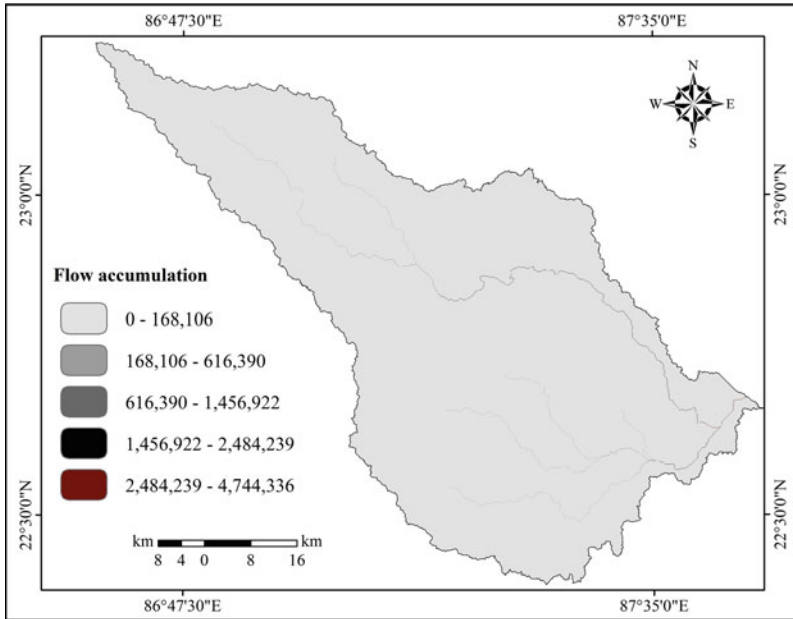
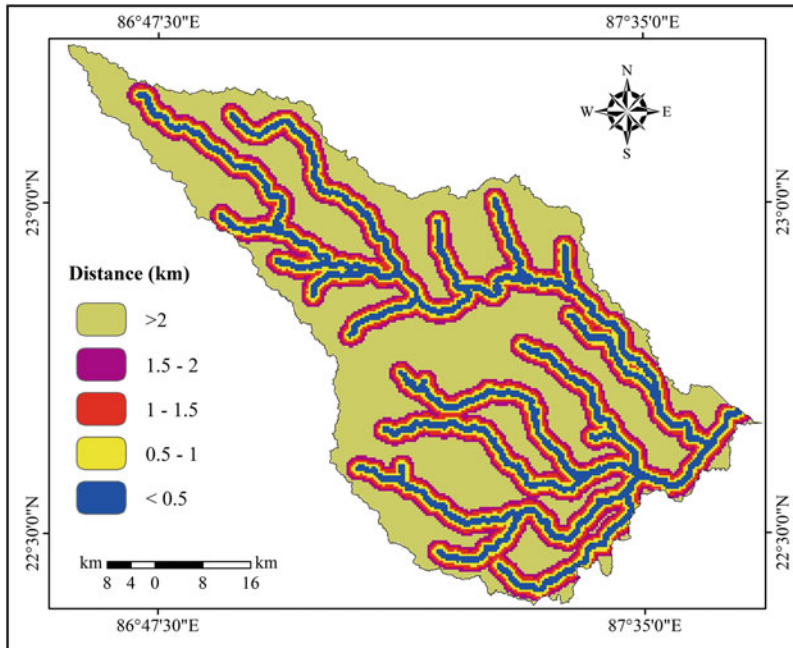**Fig. 6.6** Flow accumulation map of Silabati river basin. (Source: SRTM DEM)

Fig. 6.7 Distance of basin area from active river channel in Silabati river basin

Drainage Density

Drainage density describes the closeness of spacing of stream channels (Ghosh et al., 2020a). It is defined as the total length of streams per unit of area (Kale & Gupta, 2001; Pallard et al., 2009). The area with higher value of drainage density exhibits greater number of flow accumulation paths, and ultimately becomes more susceptible to flood (Chapi et al., 2017; Elkhrachy, 2015; Purnawali et al., 2017; Vojtek & Vojteková, 2019). In Silabati river basin, greater drainage density is observed in lower middle portion and it decreases to all directions of the basin (Fig. 6.8). The major areas lowest drainage density is noticed in the uppermost area of Silabati river basin.

Geomorphology

Geomorphology is the study of earth's landforms. Low-lying flood plains are more susceptible to flood compared to pediment–pediplain complex and denudational hills (Das, 2018; Şen, 2018). The geomorphological map of the study area is extracted in ArcGIS environment using the geomorphological map published by GSI. The map reveals that an area of 82.11% of the total basin is formed by
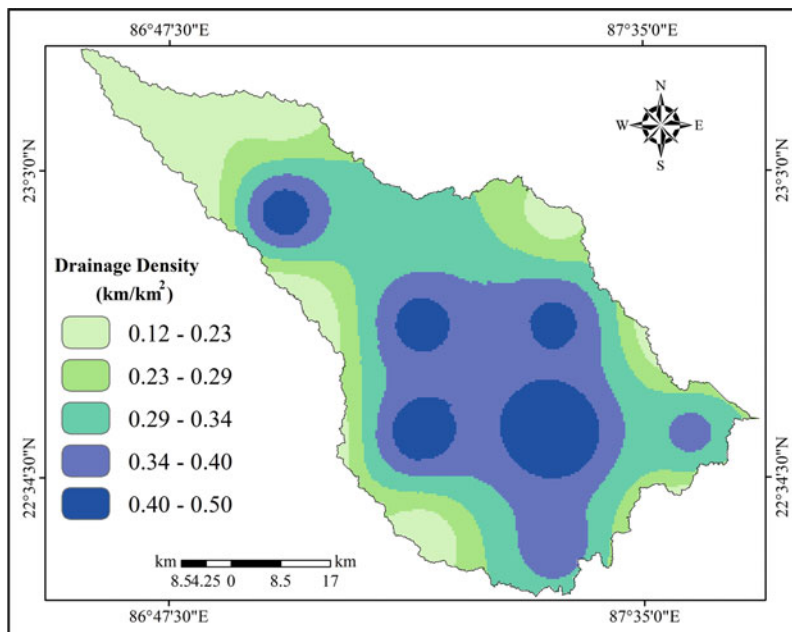

Fig. 6.8 Distribution of drainage density in Silabati river basin. (Source: SRTM DEM and Topographical map)
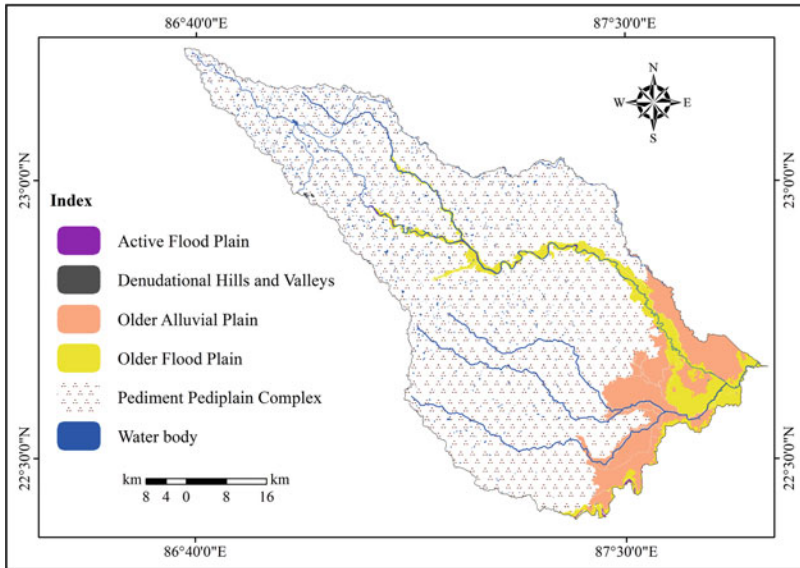
Fig. 6.9 Distribution of different geomorphological units in Silabati river basin. (Source: GSI)

pediment–pediplain complex, while 6.12% and 0.14% of areas are occupied by older flood plain and active flood plain, respectively (Fig. 6.9). Therefore, it is clear that only the lower basin area and areas along the main river channel are characterized with plain lands.

Lithology

Lithological map is used in flood susceptibility assessment due to diverse sensitivity of lithological units (Tien Bui et al., 2019). An area of hard rock lithology, many a time, is characterized by low drainage density and stream frequency (Kale & Gupta, 2001); hence the area faces less probability of being flooded (Tien Bui et al., 2019). A lithological map of the area is obtained from the District Resource Maps of GSI and processed in ArcGIS software. North-western part of the basin is covered with hard rock lithology, which is comprised of Chota Nagpur gneissic complex, Singbhum groups of rocks and metamorphosed basic rocks. Newer alluvium is found along the Silabati river and south-eastern part of the basin, while the older alluvium occupies around 70% of the total study area (Fig. 6.10).
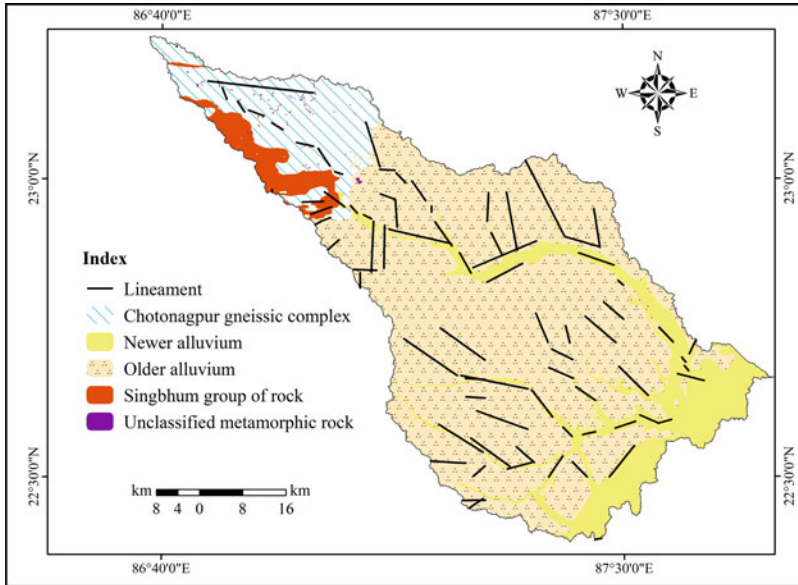
Fig. 6.10 Lithological map of Silabati river basin. (Source: GSI and https://bhuvan.nrsc.gov.in)

Surface Runoff

During precipitation, the water drains over the land surface following the local gradient and gravity. This process of water flow is called surface runoff (Uzor-Totty & Lawal, 2019). The interaction between precipitation and surface runoff depends on time and space. Surface runoff is influenced by both climatic factors (precipitation type, rainfall amount, intensity, duration, distribution, soil moisture resulting from earlier precipitation, direction of storm movement, evaporation, relative humidity, and seasons) and physical factors (vegetation, soil, elevation, slope, drainage area, basin shape, drainage network) (Uzor-Totty & Lawal, 2019). Moreover, anthropogenic activities, such as urbanization and other constructional activities, and its resultant impervious surfaces reduce the infiltration rate, increase surface runoff, and shorten runoff time into streams. Finally, all these increase the chance of higher magnitude and frequency of flood in nearby streams (Uzor-Totty & Lawal, 2019). To prepare a surface runoff map, maximum surface runoff of 4 years (2016–2019) is obtained from NRSC and interpolated using the Inverse Distance Weighted (IDW) method in ArcGIS software. At the end, the resultant map has been classified into five zones based on Jenks natural break method. The higher amount of surface runoff is recorded in the lower middle and lower reach of the basin, mainly in interfluves zones (Fig. 6.11).
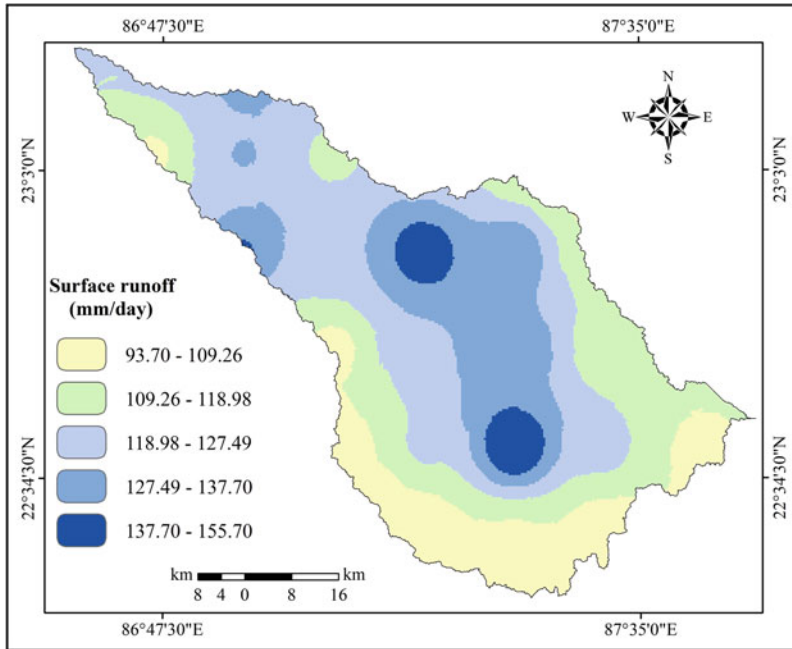
Fig. 6.11 Surface runoff map of Silabati river basin. (Source: https://bhuvan.nrsc.gov.in)

Topographic Wetness Index

Topographic wetness index is commonly used to evaluate the influence of topography in accumulation of flow or generation of runoff at any point of the basin area (Ali et al., 2019; Das, 2018, 2019; Moore et al., 1991; Sarkar & Mondal, 2020; Sørensen et al., 2006). It is expressed as TWI = ln (*a*/ tan *B*); where "TWI" refers to topographic wetness index, "*a*" is the specific basin area, and "*B*" is the local slope (Das, 2018, 2019; Sørensen et al., 2006; Tien Bui et al., 2019). The area with higher TWI value indicates high potentiality of flood event (Das, 2018; Tien Bui et al., 2019). It is evident that the higher TWI value is found in active flood plain region of Silabati river basin because of lower elevation of this area (Fig. 6.12).

Land Use Land Cover

Land use land cover has a significant role in determining surface runoff, which is directly related to flood event in catchment area (Phrakonkham et al., 2019). An area covered with vegetation reduces the intensity of surface runoff, and enhances the proliferation of infiltration process; whereas build-up area strongly impedes water percolation into the ground and hastens the surface flow (Das, 2018; Hammami et al., 2019; Roslee et al., 2018; Samanta et al., 2018; Sarkar & Mondal, 2020). To
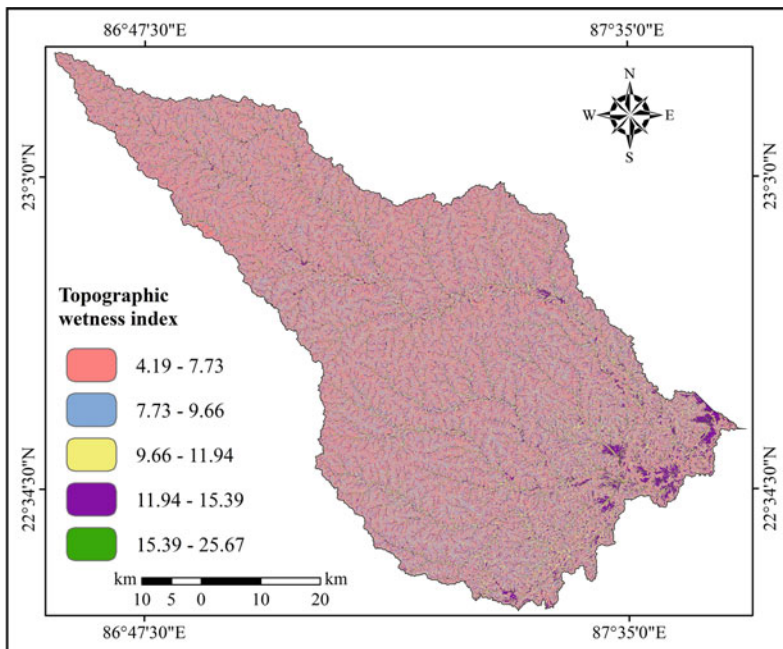
Fig. 6.12 Topographic wetness index map of Silabati river basin. (Source: SRTM DEM)

perceive the nature of land use in the study area, a supervised classification is done adopting maximum likelihood method in Erdas Imagine software (Das, 2019; Ghosh et al., 2020a; Ghosh et al., 2020b; Sarkar & Mondal, 2020). The land use pattern of Silabati river basin is dominated by agricultural land (76.79%), while forest cover is the second highest land cover occupying 20% of the total basin area. Here, Sal (Shorea Robusta), Shishu (Dalbergia), Palas (Butea Monosperma), Arjuna (Terminalia Arjuna), Sonajhuri (Acacia Auriculiformis) and Eucalyptus (Eucalyptus Globules), etc., plants are commonly found. Only 2.11% of the basin is covered by build-up area, while the water body is recorded in a tiny amount, i.e., 0.42% (Fig. 6.13).

Curvature

Curvature determines surface flow and infiltration process, and ultimately influences the incidence of flood (Das, 2018, 2019). It can be three types: (1) concave (positive curvature), (2) flat (zero curvature), and (3) convex (negative curvature). There are different opinions about the role of curvature in controlling the surface flow. Young and Mutchler (1969) advocated that a convex slope can produce much more runoff than the concave slope (Chapi et al., 2017; Young & Mutchler, 1969). Hudson and Kesel (2000) demonstrated that the area with the curvature value in between 1.0 and
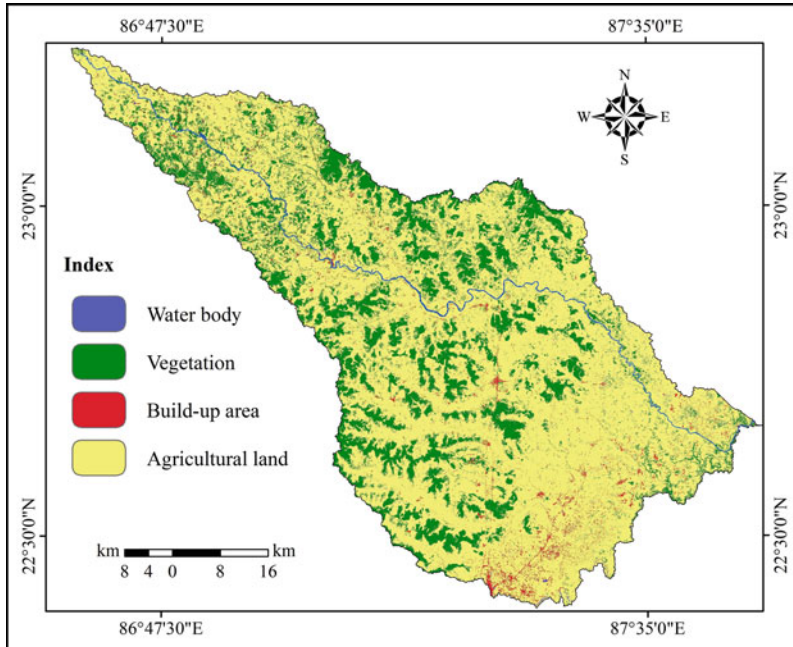
Fig. 6.13 Distribution of different types of land use land cover in Silabati river basin. (Source: Landsat 8 OLI Satellite Image)

2.0 is more vulnerable to flood (Das, 2019; Hudson & Kasel, 2000). The curvature category of −0.11 to 0.11 possesses an area of 45.72% followed by 0.11 to 0.33 (23.93%) and −0.33 to −0.11 (17.34%). It is the −2.37 to −0.33 category that shares only 2.89% of the basin area (Fig. 6.14).

Assessment of Flood Susceptibility

The final susceptibility map is generated based on integration of factor weight and sub-class rank using raster calculator in ArcGIS software. The derived map is categorized into five distinctive classes by Jenks natural break method. The classes are very high, high, moderate, low, and very low susceptibility of flood, and these classes cover 14.04%, 20.67%, 21.76%, 20.69%, and 22.84% of the total basin area, respectively (Fig. 6.15). The lower segment of the river basin is observed to be in vulnerable condition, since it belongs to the very high to high flood susceptible category. It is because the area has low elevation (6–30 m) and low slope ($<2^0$). This portion is distinguished by flat alluvial plain and well developed flood plain. The north-western part of the basin comes under very low to low flood susceptibility zone as the elevation is observed to be high (>100 m), and slope is seen more than 2^0.
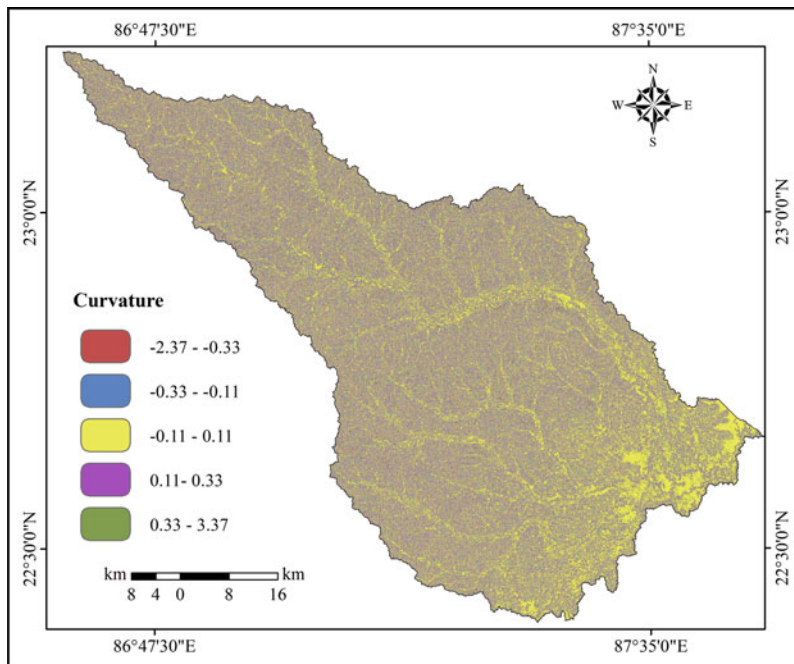
Fig. 6.14 Curvature map of Silabati river basin. (Source: SRTM DEM)

In this section, the river Silabati, flowing through the undulating topography of Chota Nagpur plateau, is characterized by narrow restricted valley, lower width-depth ratio, lacking of flood plain development, rough bed configuration and fewer number of bars; whereas the middle reach of the basin with moderate elevation shows moderate vulnerability to flood. It is observed that flood susceptibility varies from higher in south-east to lower in north-west direction (Fig. 6.15). Thus, the susceptibility of flood decreases as the elevation increases towards north-west direction.

The degree of flood vulnerability is greatly influenced by social and economic factors of an area (Działek et al., 2019). Very high and high flood susceptibility zones of the study area are mainly located at Keshpur, Ghatal, Chandrakona-I, Chandrakona-II and Daspur-I Community Development (C.D.) blocks of West Medinipur district (Fig. 6.15). Moreover, Garbeta-I, Garbeta-II, Garbeta-III, Salbani, and Medinipur C.D. blocks of West Medinipur district are also affected by flood. The population density and flood vulnerability are positively correlated to each other (Hoque et al., 2019; Sarkar & Mondal, 2020). These C.D. blocks have a population density ranging from 340 persons/km^2 to 1212 persons/km^2. High population density is found in Daspur-I (1212 persons/km^2), Ghatal (1016 persons/km^2), Chandrakona-II (819 persons/km^2), Chandrakona-I (702 persons/km^2), and Keshpur (702 persons/km^2). The Decadal (2001–2011) population growth rate varies from 13.20 to 21.37% in these blocks (Census of India, 2011). Therefore, a large number
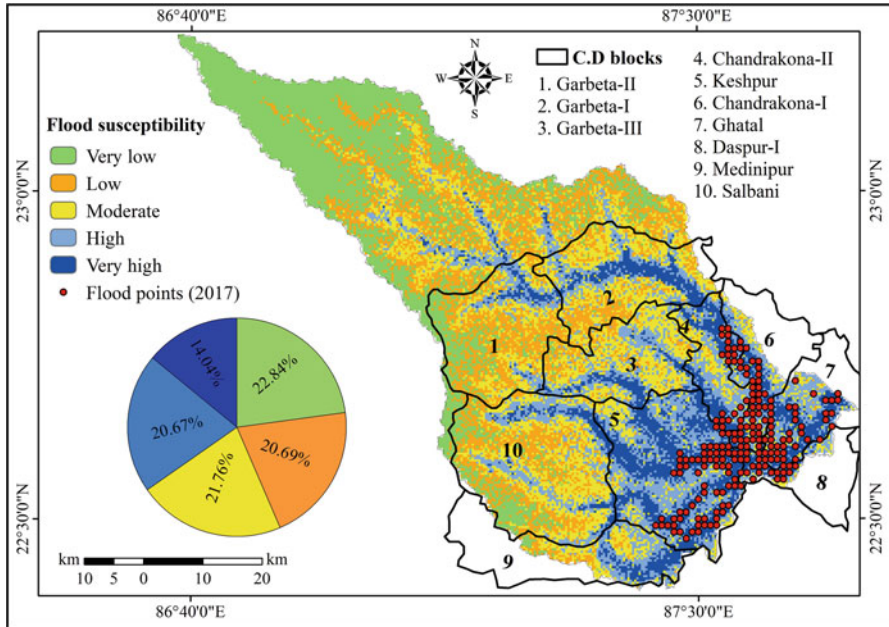
Fig. 6.15 Flood susceptibility map of Silabati river basin. The red dots in the map indicate flood points verified during 2017 flood

of people can be affected significantly by the floods. The areas with large number of households are more at-risk during occurrence of flood (Sarkar & Mondal, 2020). The household frequency ranges in between 71 and 261 households/km^2 in the studied C.D. blocks (Census of India, 2011). It is reported that the higher number of household frequency is recorded in Daspur-I (262 households/km^2), Ghatal (215 households/km^2), Chandrakona-II (175 households/km^2), Chandrakona-I (157 households/km^2), and Keshpur (142 households/km^2) (Census of India, 2011). Another important aspect needs to be mentioned here that, the flood vulnerability of an area gets momentum owing to its nature of house type (Hoque et al., 2019; Sarkar & Mondal, 2020). It is noticed that the percentage of permanent, semipermanent, and temporary houses in these C.D. blocks varies from 6.39% to 37.95%, 40.76% to 78.83%, and 8.29% to 35.38%, respectively. The large number of temporary houses is located at Medinipur (35.38%) and Keshpur (18.26%) C.D. blocks; there are significant numbers of semi-permanent houses in Chandrakona-I (78.83%), Chandrakona-II (77.92%), Keshpur (75.17%), Garbeta-II (72.05%), and Garbeta-III (71.46%) (Census of India, 2011). During flood event, children and females become more vulnerable because of their incapacitation to move at once during the emergency evacuation situations (Hoque et al., 2019). The percentage of females and children among the studied C.D. blocks ranges from 48.44% to 49.53% and 11.08% to 13.52%, respectively (Census of India, 2011).
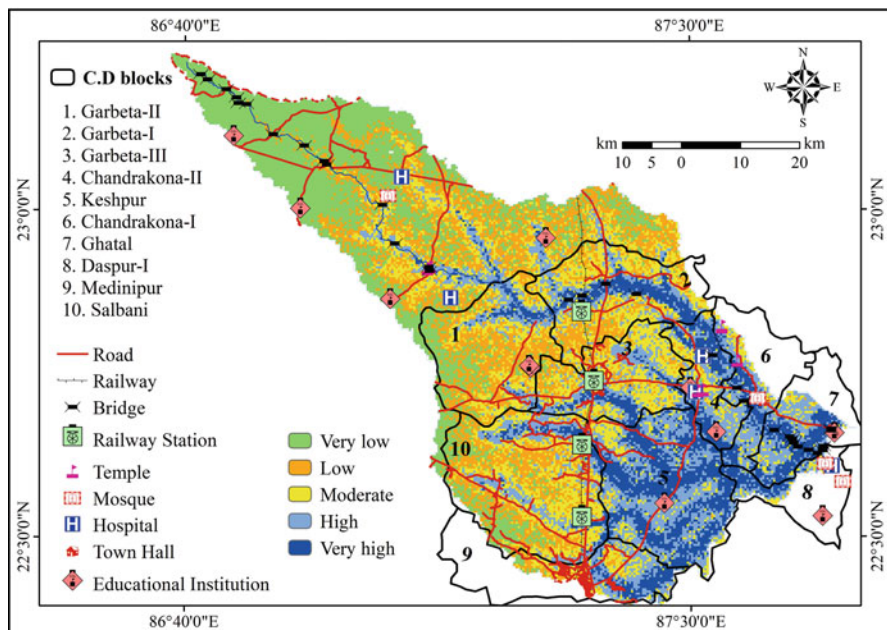
Fig. 6.16 Distribution of different socio-economic and cultural structures present within Silabati river basin overlie flood susceptibility map. (Source: Google Earth Image)

There is a negative relation between literacy rate and flood vulnerability (Hoque et al., 2019), and the average literacy rate of these C.D. blocks is calculated to be 67.28% (Census of India, 2011). The entire study area is agriculturally dependent, and flood incident brings the crop production to an end pushing thousands of men engaged in cultivation works in distress conditions (Hoque et al., 2019). It is to be noted that the agriculturally dependent populations of these C.D. blocks vary in between 59.90 and 83.67%, where the higher number of agriculturally dependent population is found in the C.D. blocks of Garbeta-II (83.67%), Chandrakona-II (83.55%), Keshpur (79.88%), Chandrakona-I (76.80%), Garbeta-I (76.37%), and Salbani (75.31%) (Census of India, 2011). There are several permanent and temporary bridges over Silabati river, and roads stretch for a considerable length within very high to moderate flood susceptibility zones (Figs. 6.16 and 6.17). Hence, it is clear that a large number of people along with many socio-economic infrastructures can significantly be affected by the flood events of Silabati river basin.

The geospatial modeling provided an effective way of flood management in the study area. Various spatial components of flood are identified and the extent of potential flooded area is quantified as well. It will facilitate the implementation of evacuation strategy, rehabilitation plan, and damage assessment during critical flood situation. It may also be effective in the development of policy, guidelines, and recommendation of land use planning.

Fig. 6.17 (**a**) Flood water spilling over the road near Bhelaidiha, Bankura on 25th July, 2017; (**b**) Flood situation near Simlapal, Bankura on 25th July, 2017 that submerged adjacent road; (**c** and **d**) Bank protection structures near Jhumka village, Bankura constructed by Irrigation & Waterways Department, Kangsabati Circle, Bankura to reduce vulnerability of river bank failure during high discharge events or floods

Validation of the Flood Susceptibility Map

In order to assess the validity of the flood susceptibility map, the AUC is computed, and the output value, i.e., 76.41% depicts that the accuracy level of the flood map prepared adopting AHP technique is well acceptable (Fig. 6.18). The value of AUC less than 50% is considered as inappropriate for flood vulnerability mapping, while the calculated value of AUC exceeding 75% is well accepted for the predicted model (Akgun et al., 2008; Egan, 1975; Ozdemir & Altural, 2013; Pedzisai, 2010; Saha, 2017; Sarkar & Mondal, 2020).
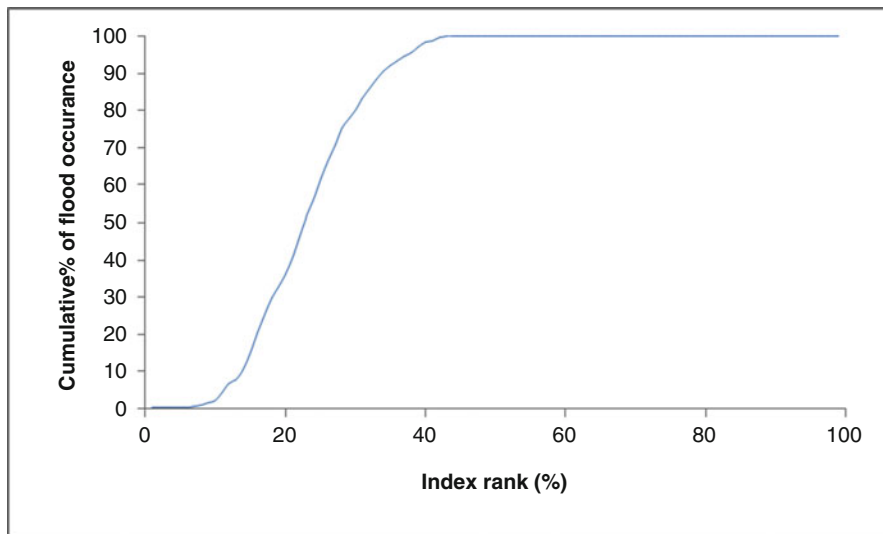
Fig. 6.18 Area under curve for validation of flood susceptibility map of Silabati river basin

6.5 Conclusion

To analyze and perceive the flood vulnerability of the Silabati river, three factors, such as elevation, slope, and flow accumulation turn out to be most dominating parameters out of adopted 11 factors considered in the present study. It is found that an area of 14.04 and 20.67% of the total basin comes under very high and high flood susceptibility zones, respectively, and most of this area lies in West Medinipur district. Amongst all C.D. blocks of the West Medinipur district, only ten are more or less affected by the flood events, but five C.D. blocks, namely: Keshpur, Ghatal, Chandrakona-I, Chandrakona-II, and Daspur-I are severely influenced by flood due to flat topography, very low elevation, and higher amount of flow accumulation compared to other C.D. blocks. As a result, a large number of populations have been witnessing and suffering from floods almost in every year for decades. Their misery is the consequences of losing shelters, crops, and cattle. To minimize the consequences of floods in Silabati river basin, implementation of different management strategies in higher flood susceptible areas is very much required. This research work may help the policy makers and implementing authorities to gather basic information related to the flood, including its vastness and areas under risk. It is suggested that C. D block level assessment of flood susceptibility can give accurate flood potentiality at local scale. Moreover, a flood simulation study can be helpful to quantify depth, velocity, and duration of flood and to access the surface water and groundwater interaction during flood.

References

Akgun, A., Dag, S., & Bulut, F. (2008). Landslide susceptibility mapping for a landslide-prone area (Findikli NE of Turkey) by likelihood-frequency ratio and weighted linear combination models. *Environmental Geology, 54*(6), 1127–1143. https://doi.org/10.1007/s00254-007-0882-8

Ali, S. A., Khatun, R., Ahmad, A., & Ahmad, S. N. (2019). Application of GIS-based analytic hierarchy process and frequency ratio model to flood vulnerable mapping and risk area estimation at Sundarban region, India. *Modeling Earth Systems and Environment, 5*, 1083–1102. https://doi.org/10.1007/s40808-019-00593-z

Anandabazar Patrika Online. (2020). *Submerged the causeway of Shilabati, the water entering the city*. Anandabazar Patrika Online.

Arya, A. K., & Singh, A. P. (2021). Multi criteria analysis for flood hazard mapping using GIS techniques: A case study of Ghaghara River basin in Uttar Pradesh, India. *Arabian Journal of Geosciences, 14*, 656. https://doi.org/10.1007/s12517-021-06971-1

Çelik, R. (2019). Evaluation of groundwater potential by GIS-based multicriteria decision making as a spatial prediction tool: Case study in the Tigris river batman-Hasankeyf sub-basin, Turkey. *Water, 11*, 2630. https://doi.org/10.3390/w11122630

Census of India. (2011). *C.D. Block Wise Primary Census Abstract Data (PCA)—West Bengal*. Directorate of Census, Government of India, New Delhi.

Chakraborty, S., & Mukhopadhyay, S. (2019). Assessing flood risk using analytical hierarchy process (AHP) and geographical information system (GIS): Application in Coochbehar district of West Bengal, India. *Natural Hazards, 99*, 247–274. https://doi.org/10.1007/s11069-019-03737-7

Chapi, K., Singh, V. P., Shirzadi, A., Shahabi, H., Bui, D. T., Pham, B. T., & Khosravi, K. (2017). A novel hybrid artificial intelligence approach for flood susceptibility assessment. *Environmental Modelling & Software, 95*, 229–245. https://doi.org/10.1016/j.envsoft.2017.06.012

Chen, Y.-R., Yeh, C.-H., & Yu, B. (2011). Integrated application of the analytic hierarchy process and the geographic information system for flood risk assessment and flood plain management in Taiwan. *Natural Hazards, 59*, 1261–1276. https://doi.org/10.1007/s11069-011-9831-7

Chowdhuri, I., Pal, S. C., & Chakrabortty, R. (2020). Flood susceptibility mapping by ensemble evidential belief function and binomial logistic regression model on river basin of eastern India. *Advances in Space Research, 65*, 1466–1489. https://doi.org/10.1016/j.asr.2019.12.003

Chung, C.-J. F., & Fabbri, A. G. (2003). Validation of spatial prediction models for landslide hazard mapping. *Natural Hazards, 30*, 451–472. https://doi.org/10.1023/B:NHAZ.0000007172.62651.2b

Dandapat, K., & Panda, G. K. (2018). A geographic information system-based approach of flood hazards modelling, Paschim Medinipur district, West Bengal, India. *Jàmbá, 10*(1), 518. https://doi.org/10.4102/jamba.v10i1.518

Dano, U., Balogun, A.-L., Matori, A.-N., Wan Yusouf, K., Abubakar, I., Said Mohamed, M., Aina, Y., & Pradhan, B. (2019). Flood susceptibility mapping using GIS-based analytic network process: A case study of Perlis, Malaysia. *Water, 11*, 615. https://doi.org/10.3390/w11030615

Das, S. (2018). Geographic information system and AHP-based flood hazard zonation of Vaitarna basin, Maharashtra, India. *Arabian Journal of Geosciences, 11*, 576. https://doi.org/10.1007/s12517-018-3933-4

Das, S. (2019). Geospatial mapping of flood susceptibility and hydro-geomorphic response to the floods in Ulhas basin, India. *Remote Sensing Applications: Society and Environment, 14*, 60–74. https://doi.org/10.1016/j.rsase.2019.02.006

Das, U., Bajpai, R., & Chakrabortty, D. (2020). River regulation and associated geo-environmental problems: A case study of lower reaches of Shilabati river basin, West Bengal, India. *International Journal of Ecology and Environmental Sciences, 2*, 233–240.

Dawod, G. M., Mirza, M. N., & Al-Ghamdi, K. A. (2011). Gis-based spatial mapping of flash flood hazard in Makkah city, Saudi Arabia. *JGIS, 03*, 225–231. https://doi.org/10.4236/jgis.2011. 33019

Deepak, S., Rajan, G., & Jairaj, P. G. (2020). Geospatial approach for assessment of vulnerability to flood in local self governments. *Geoenviron Disasters*, (7), 35.

Działek, J., Biernacki, W., Konieczny, R., Fiedeń, Ł., Franczak, P., Grzeszna, K., & Listwan-Franczak, K. (2019). Social vulnerability as a factor in flood preparedness. In *Understanding Flood Preparedness: Flood Memories, Social Vulnerability and Risk Communication in Southern Poland* (pp. 61–90). Springer International Publishing. https://doi.org/10.1007/978-3-030-04594-4_4

Egan, J. P. (1975). *Signal detection theory and ROC-analysis*. Academic.

Elkhrachy, I. (2015). Flash flood hazard mapping using satellite images and GIS tools: A case study of Najran city, kingdom of Saudi Arabia (KSA). *The Egyptian Journal of Remote Sensing and Space Science, 18*, 261–278. https://doi.org/10.1016/j.ejrs.2015.06.007

Flood Damage Statistics. (2018). State wise flood damage statistics and for the Country for the period 1953 to 2016.

Genovese, E., & Thaler, T. (2020). The benefits of flood mitigation strategies: Effectiveness of integrated protection measures. *AIMS Geosciences, 6*, 459–472.

Geological Survey of India (GSI). (2001). District Resource Map of Purulia, Bankura and Paschim Medinipur.

Ghosh, A., & Kar, S. K. (2018). Application of analytical hierarchy process (AHP) for flood risk assessment: A case study in Malda district of West Bengal, India. *Natural Hazards, 94*, 349–368. https://doi.org/10.1007/s11069-018-3392-y

Ghosh, D., Mandal, M., Karmakar, M., Banerjee, M., & Mandal, D. (2020a). Application of geospatial technology for delineating groundwater potential zones in the Gandheswari watershed, West Bengal. *Sustainable Water Resources Management, 6*, 14. https://doi.org/10.1007/s40899-020-00372-0

Ghosh, D., Mandal, M., Banerjee, M., & Karmakar, M. (2020b). Impact of hydro-geological environment on availability of groundwater using analytical hierarchy process (AHP) and geospatial techniques: A study from the upper Kangsabati river basin. *Groundwater for Sustainable Development, 11*, 100419. https://doi.org/10.1016/j.gsd.2020.100419

Government of West Bengal. (2019). *Annual flood report 2019*. Irrigation and Waterways Department.

Guha-Sapir, D., Hoyois, P., Wallemacq, P., & Below, R. (2016). *Annual disaster statistical review 2016: The numbers and trends*. CRED.

Haghizadeh, A., Siahkamari, S., Haghiabi, A. H., & Rahmati, O. (2017). Forecasting flood-prone areas using Shannon's entropy model. *Journal of Earth System Science, 126*, 39. https://doi.org/10.1007/s12040-017-0819-x

Hammami, S., Zouhri, L., Souissi, D., Souei, A., Zghibi, A., Marzougui, A., & Dlala, M. (2019). Application of the GIS based multi-criteria decision analysis and analytical hierarchy process (AHP) in the flood susceptibility mapping (Tunisia). *Arabian Journal of Geosciences, 12*, 653. https://doi.org/10.1007/s12517-019-4754-9

Hindustan Times. (2017a). *868 people killed in floods in 11 states: Govt*. Hindustan Times.

Hindustan Times. (2017b). *Bengal flood: IAF chopper winches 9 marooned villagers in dramatic rescue operation*. Hindustan Times.

Hirabayashi, Y., Mahendran, R., Koirala, S., Konoshima, L., Yamazaki, D., Watanabe, S., Kim, H., & Kanae, S. (2013). Global flood risk under climate change. *Nature Clim Change, 3*, 816–821. https://doi.org/10.1038/nclimate1911

Hong, H., Panahi, M., Shirzadi, A., Ma, T., Liu, J., Zhu, A.-X., Chen, W., Kougias, I., & Kazakis, N. (2018). Flood susceptibility assessment in Hengfeng area coupling adaptive neuro-fuzzy inference system with genetic algorithm and differential evolution. *Science of the Total Environment, 621*, 1124–1141. https://doi.org/10.1016/j.scitotenv.2017.10.114

Hoque, M., Tasfia, S., Ahmed, N., & Pradhan, B. (2019). Assessing spatial flood vulnerability at Kalapara upazila in Bangladesh using an analytic hierarchy process. *Sensors, 19*, 1302. https://doi.org/10.3390/s19061302

Huang, X., Tan, H., Zhou, J., Yang, T., Benjamin, A., Wen, S. W., Li, S., Liu, A., Li, X., Fen, S., & Li, X. (2008). Flood hazard in Hunan province of China: An economic loss analysis. *Natural Hazards, 47*, 65–73. https://doi.org/10.1007/s11069-007-9197-z

Hudson, P. F., & Kesel, R. H. (2000). Channel migration and meander-bend curvature in the lower Mississippi River prior to major human modification. *Geology, 28*(6), 531. https://doi.org/10.1130/0091-7613(2000)28<531:CMAMCI>2.0.CO;2

Inland Waterway Authority of India (IWAI). (2016). *Consultancy Services for preparation of Two Stage Detailed Project Report (DPR) of National Waterway 92, Cluster—I: Silabati River*. IWAI.

Jabbar, F. K., Grote, K., & Tucker, R. E. (2019). A novel approach for assessing watershed susceptibility using weighted overlay and analytical hierarchy process (AHP) methodology: A case study in Eagle Creek Watershed, USA. *Environmental Science and Pollution Research, 26*, 31981–31997. https://doi.org/10.1007/s11356-019-06355-9

Jahangir, M. H., Mousavi Reineh, S. M., & Abolghasemi, M. (2019). Spatial predication of flood zonation mapping in Kan River Basin, Iran, using artificial neural network algorithm. *Weather and Climate Extremes, 25*, 100215. https://doi.org/10.1016/j.wace.2019.100215

Janizadeh, S., Avand, M., Jaafari, A., Phong, T. V., Bayat, M., Ahmadisharaf, E., Prakash, I., Pham, B. T., & Lee, S. (2019). Prediction success of machine learning methods for flash flood susceptibility mapping in the tafresh watershed Iran. *Sustainability, 11*(19), 5426. https://doi.org/10.3390/su11195426

Jongman, B. (2018). Effective adaptation to rising flood risk. *Nature Communications, 9*, 1986. https://doi.org/10.1038/s41467-018-04396-1

Kale, V. S., & Gupta, A. (2001). *Introduction to geomorphology*. Orient Longman.

Kannan, V. (2010). Benchmarking the service quality of ocean container carriers using AHP. *Benchmarking, 17*, 637–656. https://doi.org/10.1108/14635771011076416

Karmakar, M., Banerjee, M., Mandal, M., & Ghosh, D. (2021). Application of AHP for groundwater potential zones mapping in plateau fringe terrain: Study from western province of West Bengal. In P. K. Shit, G. S. Bhunia, P. P. Adhikary, & C. J. Dash (Eds.), *Groundwater and society* (pp. 189–219). Springer International Publishing.

Kazakis, N., Kougias, I., & Patsialis, T. (2015). Assessment of flood hazard areas at a regional scale using an index-based approach and Analytical Hierarchy Process: Application in Rhodope–Evros region, Greece. *Science of the Total Environment, 538*, 555–563. https://doi.org/10.1016/j.scitotenv.2015.08.055

Khosravi, K., Nohani, E., Maroufinia, E., & Pourghasemi, H. R. (2016). A GIS-based flood susceptibility assessment and its mapping in Iran: A comparison between frequency ratio and weights-of-evidence bivariate statistical models with multi-criteria decision-making technique. *Natural Hazards, 83*, 947–987. https://doi.org/10.1007/s11069-016-2357-2

Khosravi, K., Shahabi, H., Pham, B. T., Adamowski, J., Shirzadi, A., Pradhan, B., Dou, J., Ly, H.-B., Gróf, G., Ho, H. L., Hong, H., Chapi, K., & Prakash, I. (2019). A comparative assessment of flood susceptibility modeling using multi-criteria decision-making analysis and machine learning methods. *Journal of Hydrology, 573*, 311–323. https://doi.org/10.1016/j.jhydrol.2019.03.073

Kowalzig, J. (2008). Climate, poverty, and justice: What the Poznań UN climate conference needs to deliver for a fair and effective global deal. *Oxfam Policy Practice Climate Change Resilience, 4*, 117–148.

Lawal, D. U., Matori, A.-N., Hashim, A. M., Yusof, K. W., & Chandio, I. A. (2012). *Detecting flood susceptible areas using GIS-based analytic hierarchy process*. IACSIT Press.

Lee, S., Lee, S., Lee, M.-J., & Jung, H.-S. (2018). Spatial assessment of urban flood susceptibility using data mining and geographic information system (GIS) tools. *Sustainability, 10*, 648. https://doi.org/10.3390/su10030648

Liuzzo, L., Sammartano, V., & Freni, G. (2019). Comparison between different distributed methods for flood susceptibility mapping. *Water Resources Management, 33*, 3155–3173. https://doi.org/10.1007/s11269-019-02293-w

Mahala, A. (2020). Land degradation processes of Silabati river basin, West Bengal, India: A physical perspective. In P. K. Shit, H. R. Pourghasemi, & G. S. Bhunia (Eds.), *Gully erosion studies from India and surrounding regions* (pp. 265–278). Springer International Publishing.

Maity, D. K., & Mandal, S. (2019). Identification of groundwater potential zones of the Kumari river basin, India: An RS & GIS based semi-quantitative approach. *Environment, Development and Sustainability, 21*, 1013–1034. https://doi.org/10.1007/s10668-017-0072-0

Malik, S., & Pal, S. C. (2021). Potential flood frequency analysis and susceptibility mapping using CMIP5 of MIROC5 and HEC-RAS model: A case study of lower Dwarkeswar River, Eastern India. *SN Applied Sciences, 3*, 31. https://doi.org/10.1007/s42452-020-04104-z

Mandal, R., & Chakrabarty, P. (2021). Badlands of gangani in West Bengal, India: An assessment on account of geotourism development. *International Journal of Geoheritage and Parks, 9*, 147–156. https://doi.org/10.1016/j.ijgeop.2021.02.001

Matori, A. N., Lawal, D. U., Yusof, K. W., Hashim, M. A., & Balogun, A.-L. (2014). Spatial analytic hierarchy process model for flood forecasting: An integrated approach. *IOP Conference Series: Earth and Environmental Science, 20*, 012029. https://doi.org/10.1088/1755-1315/20/1/012029

Mishra, K., & Sinha, R. (2020). Flood risk assessment in the Kosi megafan using multi-criteria decision analysis: A hydro-geomorphic approach. *Geomorphology, 350*, 106861. https://doi.org/10.1016/j.geomorph.2019.106861

Moore, I. D., Grayson, R. B., & Ladson, A. R. (1991). Digital terrain modelling: A review of hydrological geomorphological and biological applications. *Hydrological Processes, 5*(1), 3–30. https://doi.org/10.1002/hyp.3360050103

Murmu, P., Kumar, M., Lal, D., Sonker, I., & Singh, S. K. (2019). Delineation of groundwater potential zones using geospatial techniques and analytical hierarchy process in Dumka district, Jharkhand, India. *Groundwater for Sustainable Development, 9*, 100239. https://doi.org/10.1016/j.gsd.2019.100239

Nakajima, T., & Umeyama, M. (2015). A new concept for the safety of low-lying land areas from natural disasters. *Journal of Ocean Engineering and Marine Energy, 1*(1), 19–29. https://doi.org/10.1007/s40722-014-0002-2

Natarajan, L., Usha, T., Gowrappan, M., Palpanabhan Kasthuri, B., Moorthy, P., & Chokkalingam, L. (2021). Flood susceptibility analysis in chennai corporation using frequency ratio model. *Journal of the Indian Society of Remote Sensing, 49*, 1533–1543. https://doi.org/10.1007/s12524-021-01331-8

National Remote Sensing Centre (NRSC). (2018). Bhuvan | isro's geoportal | gateway to Indian earth observation | disaster services. In: *Bhuvan*. Retrieved May 22, 2021, from https://bhuvan-app1.nrsc.gov.in/disaster/disaster.php?id=flood_hz

News18. (2019). *Several villages are in fear of flooding due to the collapse of Shilabati dam*. News18.

Ozdemir, A., & Altural, T. (2013). A comparative study of frequency ratio weights of evidence and logistic regression methods for landslide susceptibility mapping: Sultan Mountains SW Turkey. *Journal of Asian Earth Sciences, 64*, 180–197. https://doi.org/10.1016/j.jseaes.2012.12.014

Pallard, B., Castellarin, A., & Montanari, A. (2009). A look at the links between drainage density and flood statistics. *Hydrology and Earth System Sciences, 13*(7), 1019–1029. https://doi.org/10.5194/hess-13-1019-2009

Pedzisai, E. (2010). *Rainfall-runoff modelling for flash floods in Cuongthinh catchment; Yen Bai Province: Vietnam*. International Institute for Geo-information Science and Earth Observation.

Periyasamy, A. P., Ramamoorthy, S. K., Rwawiire, S., & Zhao, Y. (2018). Sustainable wastewater treatment methods for textile industry. In S. S. Muthu (Ed.), *Sustainable Innovations in Apparel Production* (pp. 21–87). Springer, Singapore. https://doi.org/10.1007/978-981-10-8591-8_2

Phrakonkham, S., Kazama, S., Komori, D., & Sopha, S. (2019). Distributed hydrological model for assessing flood hazards in Laos. *JWARP, 11*, 937–958. https://doi.org/10.4236/jwarp.2019.118056

Pradhan, B. (2010). Flood susceptible mapping and risk area delineation using logistic regression, GIS and remote sensing. *Journal of Spatial Hydrology, 9*.

Rahman, M., Ningsheng, C., Islam, M. M., Dewan, A., Iqbal, J., Washakh, R. M. A., & Shufeng, T. (2019). Flood susceptibility assessment in Bangladesh using machine learning and multi-criteria decision analysis. *Earth Systems and Environment, 3*, 585–601. https://doi.org/10.1007/s41748-019-00123-y

Rahmati, O., Pourghasemi, H. R., & Zeinivand, H. (2016). Flood susceptibility mapping using frequency ratio and weights-of-evidence models in the Golastan Province, Iran. *Geocarto International, 31*, 42–70. https://doi.org/10.1080/10106049.2015.1041559

Roslee, R., Tongkul, F., Mariappan, S., & Simon, N. (2018). Flood hazard analysis (FHAN) using multi-criteria evaluation (MCE) in Penampang area, Sabah, Malaysia. *ASM Science Journal, 11*(3), 104–122.

Saaty, T. L. (1980). *The analytic hierarchy process: Planning, priority setting, resource allocation*. McGraw-Hill International Book Co.

Saaty, T. L. (1990). How to make a decision: The analytic hierarchy process. *European Journal of Operational Research, 48*, 9–26. https://doi.org/10.1016/0377-2217(90)90057-I

Saha, S. (2017). Groundwater potential mapping using analytical hierarchical process: a study on Md. Bazar Block of Birbhum District West Bengal. *Spatial Information Research, 25*(4), 615–626. https://doi.org/10.1007/s41324-017-0127-1

Saha, A. K., & Agrawal, S. (2020). Mapping and assessment of flood risk in Prayagraj district, India: A GIS and remote sensing study. *Nanotechnology for Environmental Engineering, 5*, 11. https://doi.org/10.1007/s41204-020-00073-1

Samanta, S., Pal, D. K., & Palsamanta, B. (2018). Flood susceptibility analysis through remote sensing, GIS and frequency ratio model. *Applied Water Science, 8*, 66. https://doi.org/10.1007/s13201-018-0710-1

Sanyal, J., & Lu, X. X. (2003). Application of remote sensing in flood management with special reference to monsoon Asia: A review. *Natural Hazards, 33*, 283–301. https://doi.org/10.1023/B:NHAZ.0000037035.65105.95

Sarkar, D., & Mondal, P. (2020). Flood vulnerability mapping using frequency ratio (Fr) model: A case study on Kulik river basin, Indo-Bangladesh Barind region. *Applied Water Science, 10*, 17. https://doi.org/10.1007/s13201-019-1102-x

Şen, Z. (2018). *Flood modeling, prediction and mitigation* (1st ed.). Springer International Publishing: Imprint: Springer.

Shafapour Tehrany, M., Kumar, L., Neamah Jebur, M., & Shabani, F. (2019a). Evaluating the application of the statistical index method in flood susceptibility mapping and its comparison with frequency ratio and logistic regression methods. *Geomatics, Natural Hazards and Risk, 10*, 79–101. https://doi.org/10.1080/19475705.2018.1506509

Shafapour Tehrany, M., Kumar, L., & Shabani, F. (2019b). A novel GIS-based ensemble technique for flood susceptibility mapping using evidential belief function and support vector machine: Brisbane, Australia. *Peer Journal, 7*, e7653. https://doi.org/10.7717/peerj.7653

Sørensen, R., Zinko, U., & Seibert, J. (2006). On the calculation of the topographic wetness index: evaluation of different methods based on field observations. *Hydrology and Earth System Sciences, 10*(1), 101–112. https://doi.org/10.5194/hess-10-101-2006

Sphere India. (2018). *Kerala floods joint detailed needs assessment report: In the aftermath of the floods in Kerala*. Sphere India Inter Agency Coordination Standard Operating Procedures (SOP).

Subbarayan, S., & Sivaranjani, S. (2020). Modelling of flood susceptibility based on GIS and analytical hierarchy process—A case study of Adayar river basin, Tamil Nadu, India. In I. Pal, J. von Meding, S. Shrestha, I. Ahmed, & T. Gajendran (Eds.), *An interdisciplinary approach for disaster resilience and sustainability* (pp. 91–110). Springer Singapore.

Swain, K. C., Singha, C., & Nayak, L. (2020). Flood susceptibility mapping through the GIS-AHP technique using the cloud. *IJGI, 9*, 720. https://doi.org/10.3390/ijgi9120720

Taylor, J., Lai, K. M., Davies, M., Clifton, D., Ridley, I., & Biddulph, P. (2011). Flood management: Prediction of microbial contamination in large-scale floods in urban environments. *Environment International, 37*, 1019–1029. https://doi.org/10.1016/j.envint.2011.03.015

Tehrany, M. S., & Jones, S. (2017). Evaluating the variations in the flood susceptibility maps accuracies due to the alterations in the type and extent of the flood inventory. *International Archives of the Photogrammetry, Remote Sensing and Spatial Information Sciences, XLII-4* (W5), 209–214. https://doi.org/10.5194/isprs-archives-XLII-4-W5-209-2017

Tehrany, M. S., Pradhan, B., Mansor, S., & Ahmad, N. (2015). Flood susceptibility assessment using GIS-based support vector machine model with different kernel types. *Catena, 125*, 91–101. https://doi.org/10.1016/j.catena.2014.10.017

Tien Bui, D., Hoang, N.-D., Pham, T.-D., Ngo, P.-T. T., Hoa, P. V., Minh, N. Q., Tran, X.-T., & Samui, P. (2019). A new intelligence approach based on GIS-based Multivariate Adaptive Regression Splines and metaheuristic optimization for predicting flash flood susceptible areas at high-frequency tropical typhoon area. *Journal of Hydrology, 575,* 314–326. https://doi.org/10.1016/j.jhydrol.2019.05.046

Uzor-Totty, A. E., & Lawal, O. (2019). Surface Runoff Dynamics across Imo River Basin: Implications for Flood Management. *Watershed Modelling & Flood Risk.* CDRMDS Regional Conference on Disaster Risk Reduction & Centre's 10th Year Anniversary: From Disaster Risk Vulnerability to Sustainability Actions

Vojtek, M., & Vojteková, J. (2019). Flood susceptibility mapping on a national scale in slovakia using the analytical hierarchy process. *Water, 11*, 364. https://doi.org/10.3390/w11020364

Wallemacq, P., & Rowena, H. (2018). *Economic losses, poverty and disasters 1998–2017*. Centre for Research on the Epidemiology of Disasters (CRED) and UNISDR.

Wanders, N., Karssenberg, D., de Roo, A., de Jong, S. M., & Bierkens, M. F. P. (2014). The suitability of remotely sensed soil moisture for improving operational flood forecasting. *Hydrology and Earth System Sciences, 18*, 2343–2357. https://doi.org/10.5194/hess-18-2343-2014

Waris, M., Panigrahi, S., Mengal, A., Soomro, M. I., Mirjat, N. H., Ullah, M., Azlan, Z. S., & Khan, A. (2019). An application of analytic hierarchy process (Ahp) for sustainable procurement of construction equipment: Multicriteria-based decision framework for Malaysia. *Mathematical Problems in Engineering, 2019*, 1–20. https://doi.org/10.1155/2019/6391431

World Disasters Report. (2015). *World Disasters Report Focus on local actors, the key to humanitarian effectiveness*. The International Federation of Red Cross and Red Crescent Societies.

World Health Organization (WHO). (2018). *Floods*. World Health Organization. Retrieved May 22, 2021, from https://www.who.int/westernpacific/health-topics/floods

Young, R. A., & Mutchler, C. K. (1969). Effect of slope shape on erosion and runoff. *Transactions of the American Society of Agricultural Engineers, 12*, 231–233.

Yousuf Gazi, M., Ashraful Islam, M., & Hossain, S. (2019). Flood-hazard mapping in a regional scale—Way forward to the future hazard atlas in Bangladesh. *Malaysian Journal Geosciences, 3*, 01–11. https://doi.org/10.26480/mjg.01.2019.01.11